Supplementary material

Behavioral paradigm used in the scanner

In the card-guessing paradigm implemented here, participants were required to guess, through a button press, whether a card with a possible value of 1-9 (excluding 5) would be lower or higher than 5. Depending on the trial type and their guess, participants could win £1 ($1.6), lose 50 pence (80 cents) or stay the same regarding their total winnings. During each trial, participants had four seconds to guess, after which the trial type was revealed: potential reward (indicated by an upwards pointing arrow) or potential loss (downwards pointing arrow). This anticipation period lasted 8, 10 or 12 seconds; and was immediately followed by the "actual" numeric value of the card (500msec) and the outcome (a green upward-facing arrow for win, a red downward-facing arrow for loss, or a yellow circle for neutral feedback; 500msec). Finally, a crosshair separated the trial from the next; this was presented for 11, 9 or 7 seconds depending on the length of the anticipation phase, so that all trials had the same total duration of 24 seconds (see supplementary Figure 1). Trials were presented in pseudorandom order with predetermined outcomes. The task included a total of 24 trials: 12 anticipation of potential reward (leading to 6 actual reward and 6 non-reward/ "disappointment" trials), and 12 anticipation of potential loss trials (leading to 6 actual loss, and 6 non-loss/"relief" trials). The participants were unaware of the fixed outcome probabilities and, despite the fact that they did not obtain any additional monetary reward for correct performance on the task, they were encouraged to perform as well as possible. The whole task lasted for 9 ½ minutes.

Figure 1

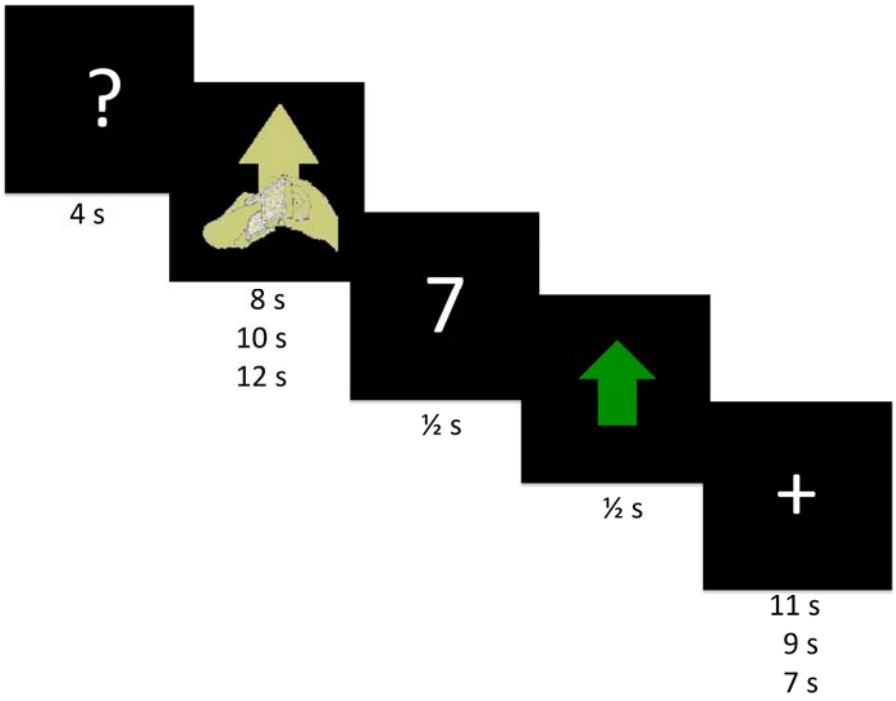

MRI data acquisition and pre-processing

During task performance, 272 brain volumes of 35 slices (3.2mm thick and AC-PC orientated) were acquired interleaved through Gradient-echo echoplanar images using a 3T General Electric HDx MRI Scanner(TR=2s;TE=35msec, flip angle=90^0; FOV=205mm; in-plane resolution=64x64; voxel size=3.2mm isotropic). Each run started with 4 dummy scans to set longitudinal magnetization into steady state.

For co-registration of fMRI data into standard space and measurement of striatal volume, a 3D FSPGR image was obtained for each participant(TR=7.9msec; TE=3.0msec; inversion time=450msec; flip angle=20^0; acquisition matrix=256(AP)x192(LR)x172(SI), 1mm isotropic voxels). Registration of fMRI data was optimized using high-resolution field-maps.

Data Supplement for Caseras et al. (doi: 10.1176/appi.ajp.2012.12020169)

fMRI data were pre-processed using the following steps: motion correction using MCFLIRT(1); non-brain removal using BET(2); spatial smoothing using a Gaussian kernel of FWHM 5mm; grand-mean intensity normalization of the entire 4D dataset; highpass temporal filtering of frequencies>0.02Hz; and registration to individual T1 anatomical images using FLIRT(3).

Structural (volumetric) MRI analysis

Structural MRI analysis was conducted using the fully-automated and widely validated Freesurfer image analysis suite (version v 4.4.0) (http://surfer.nmr.mgh.harvard.edu). The sophisticated segmentation process in Freesurfer provides anatomically accurate measurements of regional brain volumes that are superior to voxel-based morphometry and have similar advantages to manual ROI tracing, but without the potential for rater bias. The technical details of these procedures are described in prior publications (4-15). Briefly, this processing includes motion correction of volumetric T1 weighted images, removal of non-brain tissue using a hybrid watershed/surface deformation procedure (16), automated Talairach transformation, segmentation of the subcortical white matter and deep gray matter volumetric structures (including hippocampus, amygdala, caudate, putamen, ventricles)(8,9), intensity normalization (17), tessellation of the gray matter white matter boundary, automated topology correction (7,16), and surface deformation following intensity gradients to optimally place the gray/white and gray/cerebrospinal

Data Supplement for Caseras et al. (doi: 10.1176/appi.ajp.2012.12020169)

fluid borders at the location where the greatest shift in intensity defines the transition to the other tissue class (4-6) . Brain volumes in our striatal ROIs (left and right putamen and nucleus accumbens) were automatically generated for each subject following the subcortical segmentation process. We examined the putamen and nucleus accumbens segmentations as these showed the greatest overlap with the VS ROI used in the fMRI analysis. Quality control checks were conducted by visual verification of segmentation and alignment for each subject, and as a final check, we searched for and excluded any extreme outliers in regional volume measures in our striatal ROIs (there were none).

Full ANOVA and analysis of BOLD responses during punishment anticipation

The region-of-interest analysis centered in the ventral striatum showed a significant group x condition (reward anticipation v. punishment anticipation) interaction (F(2,47)=3.98, p=0.025).We therefore report here the results, both from an ROI analysis centered in the ventral striatum and whole brain analysis, of the initial 2 seconds of the punishment anticipation period. However, since we had no a-priori hypotheses regarding these analyses, these represent exploratory analyses only. The ROI analysis for punishment anticipation showed reduced ventral-striatal activity for bipolar-II compared to bipolar-I (p<.05;41voxels) and to healthy controls(p<.05;73 voxels), and no differences in ventral-striatal activity between bipolar-I and healthy controls. These findings, together with our main findings regarding between-group differences in ventral-striatal activity to reward anticipation, indicate that the above group x condition interaction observed in the ventral-striatum resulted from

Data Supplement for Caseras et al. (doi: 10.1176/appi.ajp.2012.12020169)

significantly greater ventral-striatal activity to reward anticipation, and significantly reduced ventral-striatal activity to punishment anticipation, in bipolar-II v. other groups (supplementary Figure 2).

The whole brain analysis showed reduced activity in bipolar-II participants compared to controls in the left anterior insula (x=-42, y=-12, z=6; Z=2.93, p<.05 corrected) extending into the caudate, the left ventrolateral prefrontal cortex (BA47; x=-46,y=30,z=2; Z=3.06, p<.05 corrected), and the left superior temporal cortex (BA41; x=-52, y=-20, z=8; Z=2.94, p<.05 corrected) during punishment anticipation (supplementary Figure 2).

Figure 2

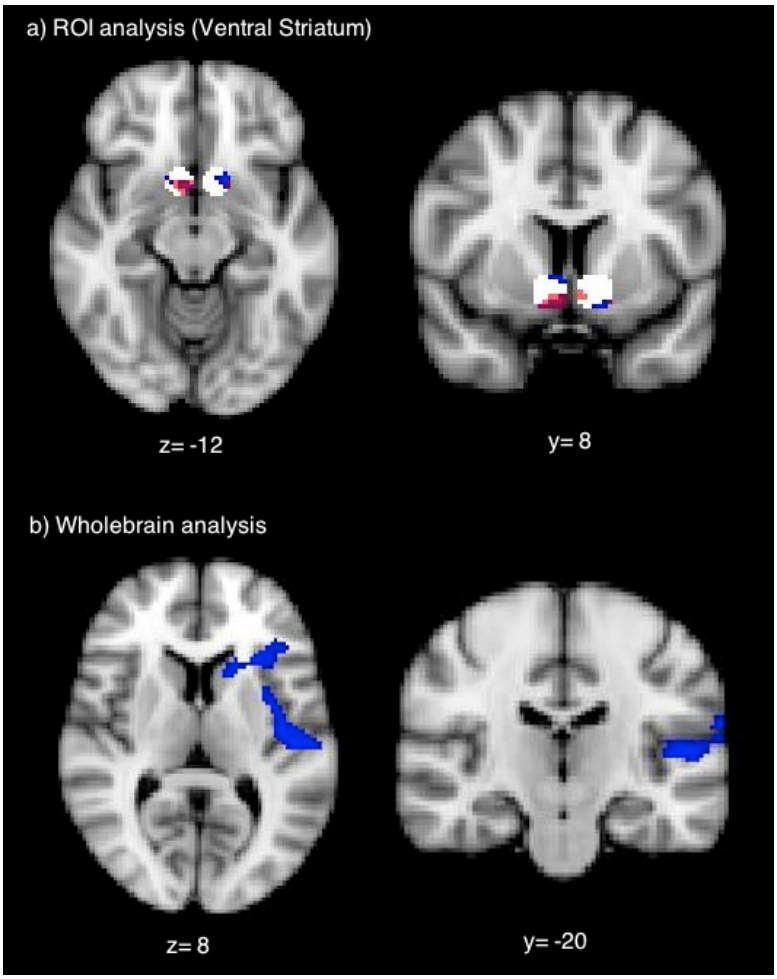

Data Supplement for Caseras et al. (doi: 10.1176/appi.ajp.2012.12020169)

References

1. Jenkinson M, Bannister P, Brady M, Smith S: Improved optimisation for the robust and accurate linear registration and motion correction of brain images. Neuroimage 2002; 17: 825-841

2. Smith S: Fast Robust Automated Brain Extraction. Hum Brain Mapp 2002; 17:143-155

3. Jenkinson M, Smith S: A global optimization method for robust affine registration of brain images. Med Image Anal 2001: 5:143-156

4. Dale AM, Fischl B, Sereno MI: Cortical surface-based analysis. I. Segmentation and surface reconstruction. Neuroimage 1999; 9:179-194

5. Dale AM, Sereno MI: Improved localization of cortical activity by combining EEG and MEG with MRI cortical surface reconstruction: a linear approach. J Cogn Neurosci 1993; 5:162-176

6. Fischl B, Dale AM: Measuring the thickness of the human cerebral cortex from magnetic resonance images. Proc Natl Acad Sci U S A 2000; 97:11050-11055

7. Fischl B, Liu A, Dale AM: Automated manifold surgery: constructing geometrically accurate and topologically correct models of the human cerebral cortex. IEEE Trans Med Imaging 2001; 20:70-80

8. Fischl B, Salat DH, Busa E, Albert M, Dieterich M, Haselgrove C, van der Kouwe A, Killiany R, Kennedy D, Klaveness S, Montillo A, Makris N, Rosen B, Dale AM: Whole brain segmentation: automated labeling of neuroanatomical structures in the human brain. Neuron 2002; 33:341-355

9. Fischl B, Salat DH, van der Kouwe AJ, Makris N, Segonne F, Quinn BT, Dale AM: Sequence-independent segmentation of magnetic resonance images. Neuroimage 2004; 23 Suppl 1:S69-84

10. Fischl B, Sereno MI, Dale AM: Cortical surface-based analysis. II: Inflation, flattening, and a surface-based coordinate system. Neuroimage 1999: 9:195-207

11. Fischl B, Sereno MI, Tootell RB, Dale AM: High-resolution intersubject averaging and a coordinate system for the cortical surface. Hum Brain Mapp 1999; 8:272-284

12. Fischl B, van der Kouwe A, Destrieux C, Halgren E, Segonne F, Salat DH, Busa E, Seidman LJ, Goldstein J, Kennedy D, Caviness V, Makris N, Rosen B, Dale AM: Automatically parcellating the human cerebral cortex. Cereb Cortex 2004; 14: 11-22

13. Han X, Jovicich J, Salat D, van der Kouwe A, Quinn B, Czanner S, Busa E, Pacheco J, Albert M, Killiany R, Maguire P, Rosas D, Makris N, Dale A, Dickerson B, Fischl B: Reliability of MRI-derived measurements of human cerebral cortical

thickness: the effects of field strength, scanner upgrade and manufacturer. Neuroimage 2006; 32:180-194

14. Jovicich J, Czanner S, Greve D, Haley E, van der Kouwe A, Gollub R, Kennedy D, Schmitt F, Brown G, Macfall J, Fischl B, Dale A: Reliability in multi-site structural MRI studies: effects of gradient non-linearity correction on phantom and human data. Neuroimage 2006; 30:436-443

15. Segonne F, Dale AM, Busa E, Glessner M, Salat D, Hahn HK, Fischl B: A hybrid approach to the skull stripping problem in MRI. Neuroimage 2004; 22:1060-1075

16. Segonne F, Pacheco J, Fischl B: Geometrically accurate topology-correction of cortical surfaces using nonseparating loops. IEEE Trans Med Imaging 2007; 26: 518-529

17. Sled, J.G., Zijdenbos, A.P., Evans, A.C., 1998. A nonparametric method for automatic correction of intensity nonuniformity in MRI data. IEEE Trans Med Imaging 17, 87-97.

Data Supplement for Caseras et al. (doi: 10.1176/appi.ajp.2012.12020169)

Figure Legends

Supplementary Figure 1. Event-related card guessing paradigm. This figure depicts one trial corresponding to 'potential reward'. Participants made their guess of "higher or lower than 5" by pressing with either the index or middle finger during the presentation of the question mark. The anticipation period corresponds to the presentation of shuffling cards with an arrow pointing upwards (potentially winning trial). The actual value of the card (slide with a number between 1-9 excluding 5) and the green arrow pointing upwards taken together correspond to the outcome phase (in this case indicating win) and totalling one second presentation. A fixation crosshair was presented at the end of each trial and was modelled as the baseline. The numbers under each slide indicate the time in seconds for each event within the trial. The anticipation period had a duration of 8, 10 or 12 seconds, associated with a crosshair period of 11, 9 or 7 seconds respectively, resulting in a total duration of 24 seconds for each trial. The MRI acquisition was time-locked (TR= 2 seconds) to the beginning of each trial.

Supplementary Figure 2. Group differences in (a) ventral-striatal activity (blue: healthy controls > bipolar-II; red: bipolar-I > bipolar-II) and (b) left ventrolateral prefrontal cortex, anterior insula, caudate and superior temporal cortex (healthy controls > bipolar-II), during the initial 2 seconds of the anticipation of punishment period.

Data Supplement for Caseras et al. (doi: 10.1176/appi.ajp.2012.12020169)